Accepted Manuscript

Raster-Scanning Optoacoustic Mesoscopy for Gastrointestinal Imaging at High Resolution

Ferdinand Knieling, Jean Gonzales-Menezes, Jing Claussen, Mathias Schwarz, Clemens Neufert, Fabian B. Fahlbusch, Timo Rath, Oana-Maria Thoma, Viktoria Kramer, Bianca Menchicchi, Christina Kersten, Kristina Scheibe, Sebastian Schürmann, Birgitta Carlé, Wolfgang Rascher, Markus F. Neurath, Vasilis Ntziachristos, Maximilian J. Waldner

PII: S0016-5085(18)30011-8
DOI: 10.1053/j.gastro.2017.11.285
Reference: YGAST 61608

To appear in: *Gastroenterology*
Accepted Date: 28 November 2017

Please cite this article as: Knieling F, Gonzales-Menezes J, Claussen J, Schwarz M, Neufert C, Fahlbusch FB, Rath T, Thoma O-M, Kramer V, Menchicchi B, Kersten C, Scheibe K, Schürmann S, Carlé B, Rascher W, Neurath MF, Ntziachristos V, Waldner MJ, Raster-Scanning Optoacoustic Mesoscopy for Gastrointestinal Imaging at High Resolution, *Gastroenterology* (2018), doi: 10.1053/j.gastro.2017.11.285.

Raster-Scanning Optoacoustic Mesoscopy for Gastrointestinal Imaging at High Resolution

Ferdinand Knieling[1,2], Jean Gonzales-Menezes[2], Jing Claussen[3], Mathias Schwarz[3], Clemens Neufert[2], Fabian B Fahlbusch[1], Timo Rath[2,4], Oana-Maria Thoma[2,8], Viktoria Kramer[2], Bianca Menchicchi[2], Christina Kersten[2], Kristina Scheibe[2], Sebastian Schürmann[5], Birgitta Carlé[5], Wolfgang Rascher[1], Markus F Neurath[2,4], Vasilis Ntziachristos[6,7], Maximilian J Waldner[2,8]

1 Department of Pediatrics, Friedrich-Alexander-Universität Erlangen-Nürnberg, Germany
2 Department of Medicine 1, Friedrich-Alexander-Universität Erlangen-Nürnberg, Germany
3 iThera Medical GmbH, München
4 Ludwig Demling Center of Excellence, Friedrich-Alexander-Universität Erlangen-Nürnberg, Germany
5 Institute of Medical Biotechnology, Friedrich-Alexander-Universität Erlangen-Nürnberg, Germany
6 Helmholtz Zentrum München, Institute for Biological and Medical Imaging, Germany
7 Munich School of Bioengineering, Technische Universität München, Germany
8 Erlangen Graduate School in Advanced Optical Technologies (SAOT), Friedrich-Alexander-Universität Erlangen-Nürnberg, Germany

Corresponding author:
Maximilian J. Waldner, MD
Department of Medicine 1
Friedrich-Alexander-Universität Erlangen-Nürnberg
Ulmenweg 18
91054 Erlangen, Germany
Email: maximilian.waldner@uk-erlangen.de

Contributions

FK, MJW study concept and design, drafting of the manuscript, and interpretation of the data; FK, MJW, JC data analysis; FK, BC, JC acquisition of the data; JGM, FBF, TR, OMT, VK, BM, CK, KS, SS technical or material support, all authors critical revision of the manuscript for important intellectual content, MJW study supervision

Conflict of interest

JC and MS are employees of iThera Medical. All other authors disclose no conflicts of interest.

Activities not related to the article: FK and MJW received travel expenses for scientific meetings from iThera Medical GmbH, Germany VN is a shareholder of iThera Medical. Other relationships: VN has US 20140198606 A1 / EP2754388A1, WO 2012103903 A1, WO 2011000389 A1, EP2148183, PCT/EP2008/006142, and US 61/066,187; PCT/EP2009/001137 patents issued and patent WO201109810 1A1, PCT/EP2010/006937 licensed by SurgOptics B.V.

Acknowledgements

OMT and MJW gratefully acknowledges funding of the Erlangen Graduate School in Advanced Optical Technologies (SAOT) by the German Research Foundation (DFG) in the framework of the German excellence initiative, and funding by the German Research Foundation (DFG) within the Klinische Forschergruppe 257 (KFO 257) and Forschergruppe 2438 (FOR 2438). MFN gratefully acknowledges funding by the Emerging Fields Initiative of the Friedrich-Alexander-Universität Erlangen-Nürnberg and by the German Research Foundation (DFG) within Collaborative Research Center 1181 “Checkpoints for resolution of inflammation”. This project has received funding from the European Union’s Horizon 2020 research and innovation program under grant agreement No 732720 (ESOTRAC). The authors thank Andrea Hartner for support during study execution.

Introduction

In vivo optical imaging modalities are mostly limited to cell cultures, superficial tissues and intravital imaging since they lack either resolution or penetration depth.[1] In contrast, optoacoustic (OA) imaging – combining features of optical and ultrasound imaging - has already been used to visualize hemoglobin in depths of ~3cm in patients with Crohn's disease.[2, 3]

Realizing an even higher resolution, Raster-Scanning Optoacoustic Mesoscopy (RSOM) provides intrinsic optical tissue contrast down to 10-20µm resolution at still high penetration depths of several millimeters.[4, 5]

In this article, with its accompanying videos, we demonstrate the capability of RSOM to perform high resolution *in vivo* gastrointestinal imaging and explore its potential clinical use.

Description of the Technology

The imaging technology is integrated into a OA small animal scanner that builds upon a RSOM system (RSOM Explorer P50, iThera Medical GmbH, München, Germany) (figure 1+B).[5, 6] It uses a custom-made spherically focused LiNbO3 detector (center frequency: 50MHz, bandwidth: 10-90MHz, focal diameter: 3mm, focal distance: 3mm, f-number: 1). The recorded data are amplified by a low noise amplifier of 63dB gain. The illumination is generated by a 532nm diode pumped solid state laser (pulses: 1ns, up to 1mJ/pulse, repletion rate: 2kHz). The laser light is delivered through a customized two arm fiber bundle (spot size: 3.5mmx5mm). The scanning head is attached to two motorized stages, enabling raster scanning over a field of view (FOV) up to 15mmx15mm (step size: 20µm). The scan head is coupled to the sample surface by an interchangeable water-filled (2ml) interface. The recorded data is reconstructed with a beam-forming algorithm, which models the sensitivity field of the focused detector.[6-8]

Video Description

The first video gives an overview of light- and soundwave-based imaging technologies which are currently used or in translation for high resolution imaging. It explains how RSOM combines optical and ultrasound imaging to provide excellent specifications for preclinical and translational gastrointestinal imaging.

Then, the principle of OA imaging is explained. It is based on the illumination of tissue with pulsed laser light at 532nm. The light gets absorbed by tissue chromophores, which undergo thermoelastic expansion followed by the generation of pressure waves that are detected. Taking a freshly excised liver as an example, we demonstrate the ability of RSOM to visualize the vasculature of organs (green: small vessels, red: big vessels) without any label (figure 1C-E).

In the second video, we then show label free-images of freshly excised murine colons bearing inflammation and tumors to visualize neovascularization in neoplastic tissues. The capability of RSOM for non-invasive *in vivo* transabdominal imaging in mice is demonstrated. The increased vasculature of the colon wall during inflammation is compared to healthy specimen (figure 2A-D). In an adoptive T cell transfer colitis model, we provide the evidence that RSOM could non-invasively detect structures resembling injected labeled T cells infiltrating into the colon wall of mice with colitis.

Take Home Message

We demonstrate that RSOM allows non-invasive imaging at high resolution *in vivo*. In contrast to other optical imaging modalities, this technology is not generally restricted to the application of exogenous dyes. As we used a single wavelength laser for illumination, the integration of multiple wavelengths could further enable the label-free determination of hemoglobin oxygenation, of further tissue molecules (e.g. collagens), and a broader range of fluorescent dyes or proteins.

In the future, the integration in endoscopic devices might allow the label-free visualization of multiple, deeper layers of the intestinal wall at single cell resolution.

Figure legends

Figure 1:

A: Technical setup. **B:** Imaging principle. **C:** Low frequency (10-30MHz) detection of freshly excised liver tissue. **D:** High frequency (30-90MHz) detection. **E:** 3D-volume overlay. Bars: 1mm, XY-box: 8mm

Figure 2:

In vivo RSOM imaging from healthy and inflamed mice. The images are reconstructed from single image planes of the murine colon (max depth: 3mm).

Detected signals originate from hemoglobin (10-90MHz). **A:** *In vivo* imaging from healthy mice; Full projections (FP) YZ, XY und XZ. **B:** 3D-volume. **C:** *In vivo* imaging from colitis; FP YZ, XZ und XZ. **D:** 3D-volume. Bars: 1mm, XY-box: 8mm

Literature

1. Ntziachristos V. Nat Methods 2010;7:603-14.
2. Knieling F, et al. N Engl J Med 2017;376:1292-1294.
3. Waldner MJ, et al. Gastroenterology 2016;151:238-40.
4. Ntziachristos V, et al. Chem Rev 2010;110:2783-94.
5. Omar M, et al. Neoplasia 2015;17:208-14.
6. Omar M, et al. Opt Lett 2014;39:3911-4.
7. Schwarz M, et al. IEEE Transactions on Medical Imaging 2017.
8. Schwarz M, et al. J Biophotonics 2015.

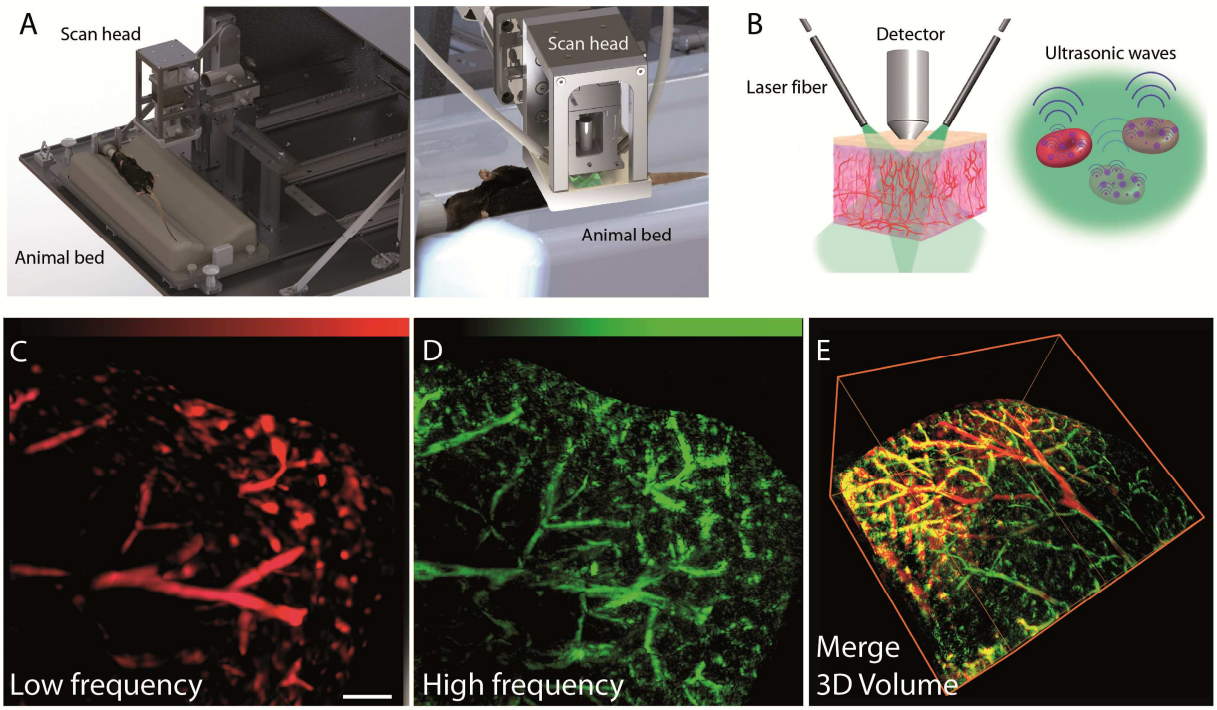

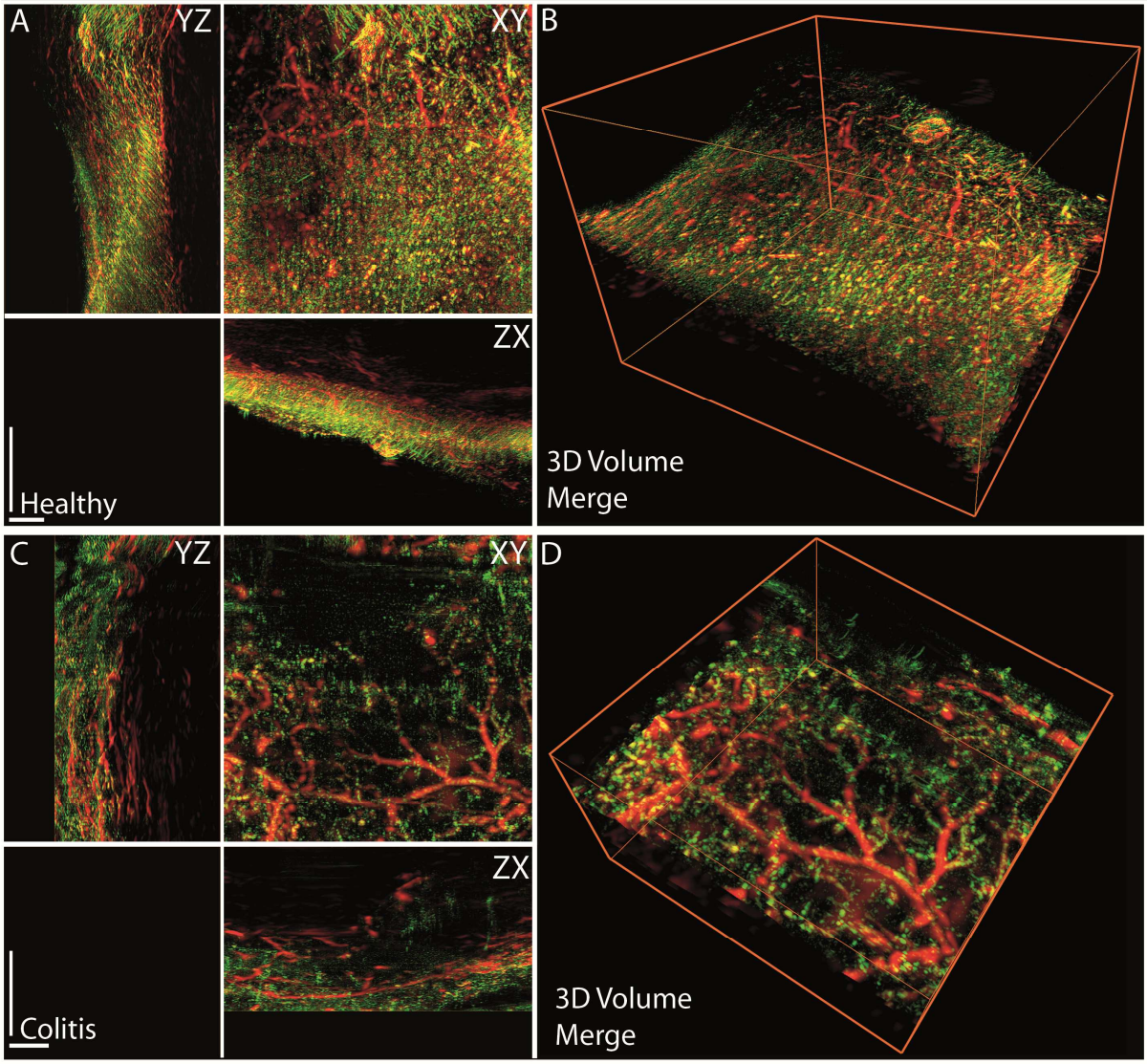
A
YZ
XY
ZX
Healthy
B
3D Volume
Merge
C
YZ
XY
ZX
Colitis
D
3D Volume
Merge

Supplementary material and methods

Knieling et al.

Raster-Scanning Optoacoustic Mesoscopy for Gastrointestinal Imaging at High Resolution

Supplementary material and methods

Tissue preparation

For fresh tissue, C57B6/J mice were sacrificed and organs were immediately transferred into phosphate buffered saline (PBS, Sigma-Aldrich Chemie GmbH, Germany). RSOM imaging was performed without any further preparation and within less than one hour.

Isolation of Primary Cells

$CD4^+CD25^-$ T cells were isolated from murine splenocytes by MACS magnetic bead separation ($CD4^+$ T Cell Isolation Kit, CD25-PE Kit, Miltenyi Biotec, Bergisch Gladbach, Germany) to a purity degree >95%.

Labeling of Primary Cells

Before further experiments, $CD4^+CD25^-$ T cells were labeled with CellTrace Yellow (Life technologies, USA) according to manufactures instructions. First, a CellTrace stock solution (5mM CellTrace in DMSO) was prepared. Then, 1µL of stock solution was added to each mL of cell suspension. This was incubated for 20 minutes at 37℃ and protected from light. Next, culture medium (RPMI, Sigma-Aldrich, Germany) was added to the cells (five times of the original staining volume) and it was incubated for 5 minutes. Finally, the cells were centrifuged and resuspended in fresh pre-warmed complete culture medium and incubated for at least 10 minutes before further experiments.

Models of colitis and colitis associated cancer (CAC)

All animal studies were conducted at the University of Erlangen-Nuremberg and approved by the Institutional Animal Care and Use Committee of the State Government of Middle Franconia. All mice were bred and maintained in individually ventilated cages.

Adoptive Transfer Colitis. Freshly isolated $CD4^+CD25^-$ splenocytes T cells (2.8×10^6) from gender-matched C57BL/6 mice (12 weeks old) were administered intraperitoneally into $RAG^{-/-}$ mice in 200µL of phosphate buffered saline.[1]

Chemically Induced Colitis and CAC. C57BL/6 mice (8–10 weeks) were obtained from the central animal facility of Erlangen. Colitis and CAC was induced as previously described.[2] For acute colitis, mice received one week of 1.8% dextran sodium sulfate (DSS, MP Biomedicals LCC, Canada) in the drinking water. For chronic colitis, mice were provided with three cycles of 1.8% DSS in the drinking water for 1 week followed by normal drinking water for 2 weeks. For CAC, mice were injected with a single dose of the mutagenic agent 7.4 mg/kg Azoxymethane (AOM, Sigma-Aldrich, Germany), followed by three similar cycles of 1.8% DSS in drinking water for 1 week followed by normal drinking water for 2 weeks.

Image reconstruction

To enhance high-frequency signal of small structures, the acquired signals were divided into two frequency bands, 10–30 MHz (low) and 30–90 MHz (high) before reconstruction.[3, 4] In the final images, an overlay of the low-frequency reconstruction (red) and high-frequency reconstruction (green) is shown. Additionally, we performed a reconstruction of the frequency band 85-87 MHz, which filters out anatomical structures with very high frequency content in order to detect signals which potentially came from the labelled cells.

Motion correction

For in vivo applications a motion correction processing was applied as previously described by Schwarz et al.[5] Briefly, the algorithm is based on the observation of disruptions of the ultrasound wave front generated by periodic vertical movements of the melanin containing skin layer. These disruptions are used to generate a smooth synthetic surface. Subsequently, the offset between these two surfaces is used to correct for the relative position of the detector (Supplementary Figure 1).

Image visualization

For image 3D visualization, the commercially available software platform Amira (FEI, ZIB; Berlin) was used. Maximum Intensity Projections and 3D images were generated using standard Amira tools. Different frequencies were pseudo-coloured and overlayed with the software. Images were sharpened using the software provided unsharp mask filter. Single fibroblast cells were highlighted by using the segmentation tool on the image stack in which signals were filtered from 30-90MHz.

All images were adjusted in hue and saturation using Photoshop elements (Adobe; San Jose) on the entire image without adding or changing features.

Multiphoton Microscopy

Ex vivo multicolor multiphoton microscopy (MPM) with spectral separation was performed on corresponding murine colonic tissues sections as described previously.[6] Briefly, an upright system (TriM-Scope II; LaVision BioTec GmbH, Germany) equipped with a femtosecond Ti-Sa-laser and a HC Fluotar L25x/0,95 W Visir objective (Leica, Germany) was used to detect signals in three photomultiplier tubes (PMT): second generation harmonics (SHG) at 395-415nm (collagens, blue); autofluorescence in the ranges of 415-485nm (NADH, green) and 540-580nm (FAD, red).

Quantification of vessel diameter and blood volume

Vessel diameter and volumes were calculated from raw images in triplicate. The blood volume was calculated using ImageJ 3D manager plugin (public-domain Java-based image processing software available at https://imagej.nih.gov). Differences were tested with two-sided Student's t-test and p-values <0.05 were considered as statistically significant.

Quantification of labeled primary cells

For quantification of labelled $CD4^+CD25^-$ T cells ex vivo and in vivo, the open-source software Icy (version 1.9.1.0) was used. By using the detection plugin 'Spot detector' with adjusted filter settings, bright spots of a certain size which most likely correspond to the labelled cells were automatically counted in the entire image or single ROIs. For quantification of bright spots in the multiphoton images, the following settings were used: Detected bright spot, Scale 2 90 (3px) and Scale 3 90 (7px), Size filter: 10-3000. For quantification of bright spots in RSOM images from the reconstruction in the frequency band 85-87 MHz, the following settings were used: detected bright spot, scale 1 (1px), size filter: 30-60. For comparison of multiple groups ANOVA with Bonferroni post-test was used. P-values <0.05 were considered as statistically significant.

Supplementary figure legends

Supplementary Figure 1:

A: Schematic overview of dimensional orientation and skin line movements/discontinuation during motion. **B:** Skin surface raw data before motion correction. **C:** Skin surface raw data after motion correction. **D:** RSOM image of murine intestine before motion correction. **E:** RSOM image of murine intestine after motion correction. Blue boxes indicate area of magnified panel in the upper left corner.

Literature

1. Powrie F,, et al. Immunity 1994;1:553-62.
2. Neufert C, et al. Nat Protoc 2007;2:1998-2004.
3. Omar M, et al. Neoplasia 2015;17:208-14.
4. Aguirre J, et al. Nature Biomedical Engineering 2017;1:0068.
5. Schwarz M, et al. Sci Rep. 2017 Sep 4;7(1):10386.
6. Schurmann S, et al. Gastroenterology 2013;145:514-6.

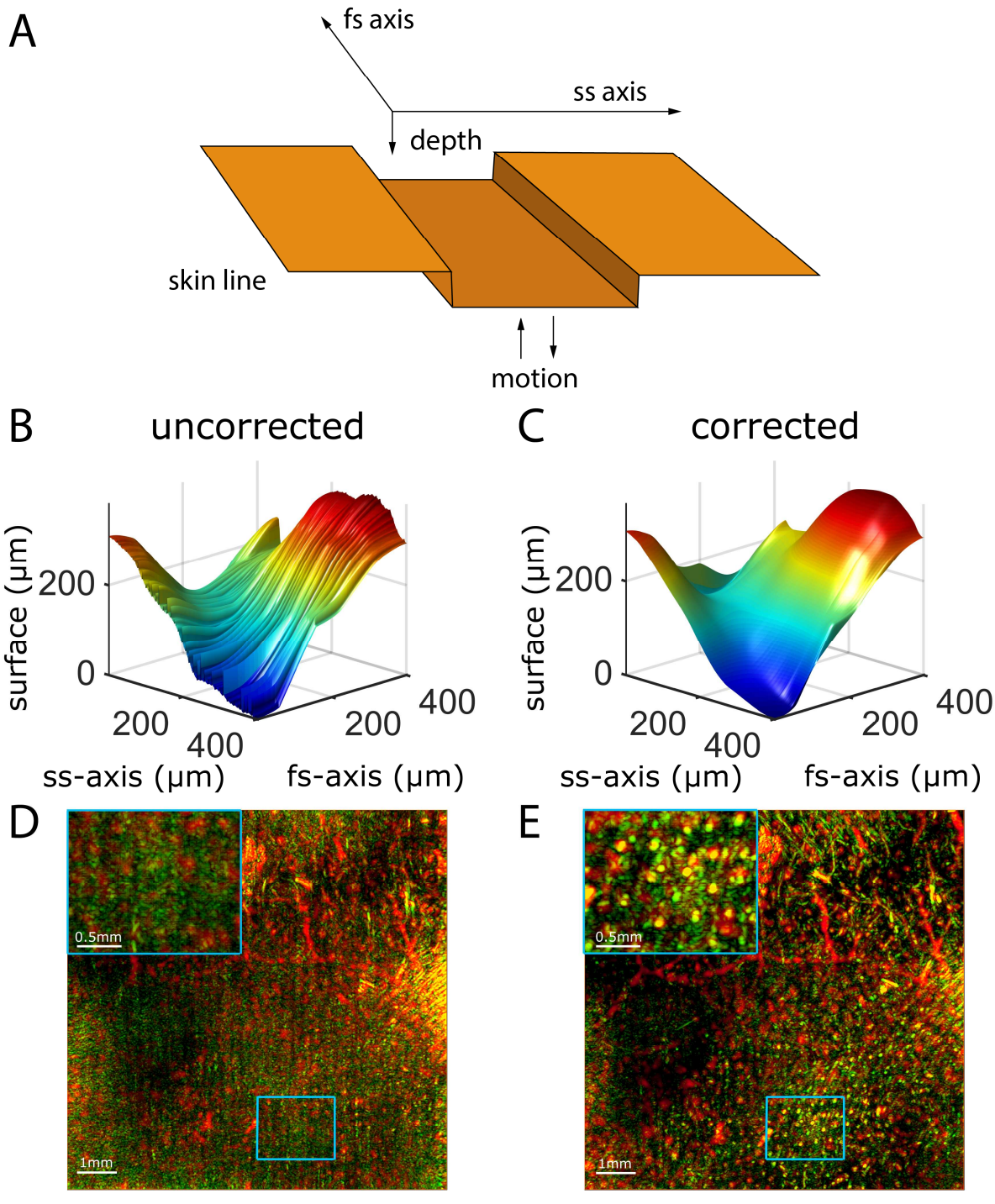
A
fs axis
ss axis
depth
skin line
motion
B
uncorrected
C
corrected
surface (µm)
200
0
200
400
ss-axis (µm)
200
400
fs-axis (µm)
D
E
0.5mm
1mm